Supporting Information

Stabilisation of iron-oxo dimers in a natural layered clay for efficient photocatalysts comparable to TiO_2

Hamza El-Hosainy, Ezz-Elregal M. Ezz-Elregal, Shinichiro Takano, Takumi Miyakage, Duotian Chen, Chenxi He, Takashi Toyao, Ken-ichi Shimizu, Akio Iwanade, Yusuke Ide and Tomohiko Okada

Corresponding author:

Yusuke Ide (IDE.Yusuke@nims.go.jp)

Tomohiko Okada (tomohiko@shinshu-u.ac.jp)

Characterisations. The amount of Fe in the products was determined by analysing dissolved samples using inductively coupled plasma–optical emission spectroscopy (Agilent 5800 spectrometer). 5 mg of sample was weighed and transferred into PFA beaker. 20 mL of HNO_3 (1+1) and 2 mL of HF were added into the beaker and decomposed by heating. After cooling, the solution was poured into 250 mL of PP volumetric flask and then 10 mL of 50 mg/L Mn standard solution was added into the flask as internal standard. This solution was diluted to marked line with Milli-Q water. XRD patterns of the products were recorded using a diffractometer (Rigaku Miniflex600/PC) equipped with a Cu Kα radiation source at 40 kV, 15 mA, and a scan rate of $2° \text{ min}^{-1}$. UV–vis diffuse reflectance spectra were recorded on a spectrophotometer (UV-2600i, Shimadzu) equipped with a Shimadzu ISR-2600Plus integrated sphere attachment. XANES and EXAFS spectra were recorded in transmission mode at the beamline BL01B1 of SPring-8 facility at the Japan Synchrotron Radiation Research Institute (JASRI; 8 GeV, 100 mA). The data analysis of the XAS spectra were performed using the Demeter software package.[1]

Formic acid oxidation. 15 mg of powder sample was mixed with 5 mL of an aqueous solution containing formic acid (5 vol%) in a Pyrex glass test tube, which was then bubbled with O_2 (purity > 99.8%) for 30 min. The test tube was sealed with a rubber septum, ultrasonicated for 2 min and then irradiated with a solar simulator (San-Ei Electric XES-155S1, $\lambda > 300$ nm, 1000 W m^{-2}) while being stirred. The headspace gas was extracted using a gas-tight syringe and analysed with a gas chromatograph (Shimadzu BID-2010 plus) equipped with a micropacked column (ShinCarbon ST).

Formaldehyde oxidation. 15 mg of powder sample was dispersed in ethanol in a glass-made petri dish (inner diameter of 27 mm) and dried at 110°C. The petri dish was placed in a stainless-made closed reactor equipped with a Pyrex glass (500 mL). 300 μmL of formalin (35%, Nacalai Tesque) was injected into the reactor and the irradiation was started after the vaporisation of formalin. The amount of CO_2 evolved was measured by a Shimadzu BID-2010 plus gas chromatograph.

DFT calculations details. All structural and energy calculations were carried out based on the spin-polarised DFT method using the Vienna Ab initio Simulation Package (VASP.5.4.4).[2,3] The core-valence electron interactions were described using the projector augmented wave method.[4] The Perdew–Burke–Ernzerhof functional[5] was used to account for structural relaxation, whereas the DFT-D3 method and the Becke–Johnson damping dispersion correction were adopted to account for dispersion interactions.[6,7] For the model structure construction, firstly, the intralayer Na^+ ions of the parent clay structure were replaced by H^+. The atomic positions were optimised while maintaining fixed lattice constants and unit cell geometry ($Al_5Si_7O_{24}H_5$: a = 5.18 Å, b = 8.98 Å, c = 15.0 Å, α = β = γ = 90°). Subsequently, to introduce aqua–Fe(III) species into the layer, a 2 × 2 × 1 super cell (see **Fig. S3**) was constructed, and both the lattice parameters and atomic positions were optimised ($Al_{20}Si_{28}O_{96}H_{20}$: a = 10.36 Å, b 17.96 Å, c = 17.0 Å, α = β = γ = 90°). Finally, aqua–Fe(III) species such as mononuclear species $[Fe^{III}(OH)(H_2O)_3]$ and dinuclear species $[(H_2O)_2Fe^{III}O_2Fe^{III}(H_2O)_2]$ and $[(H_2O)_2Fe^{III}(OH)_2Fe^{III}(H_2O)_2]$) were introduced into the layer. The atomic positions were optimised, and the total energy *E* was calculated under fixed lattice parameter and unit cell geometry conditions. Three spin multiplicities (1/2, 3/2 and 5/2) were examined for each Fe atom by specifying the initial settings for the calculations (See **Table S3**). Note that the interlayer distance was modelled to match the experimentally obtained values from XRD. The effective *U* value for Fe was set at 5.3 eV. All periodic models were calculated with a 1 × 1 × 1 k-point mesh and an energy cut-off of 400 eV. The criterion for convergence is that the maximum Hellmann−Feynman force should be less than 0.03 eV/Å.

***Ab initio* thermodynamic analysis.** *Ab initio* thermodynamic analyses[8] were performed to elucidate the effects of H_2O (liquid and gas) and temperature on the aqua–Fe(III) species in the smectite clay (the considered structures are shown in **Fig. S1**). The enthalpy and entropy at various temperatures and standard pressure (1 atm) were obtained from available NIST-JANAF Thermochemical Tables.[9] The energies of the H_2O and $Fe^{2+}(H_2O)_3(OH)$ (denoted as Fe complex) species were determined based on a large empty unit cell (25 × 25 × 25 Å^3) to mimic isolated species. The equilibrium reaction, change in energy (ΔE), Gibbs free energy (ΔG), and change in chemical potential ($\Delta\mu$) under a H_2O (liquid and gas) atmosphere are defined in Eqs. (1), (2), (3), and (4), respectively:

$$x\text{Fe complex} + \text{Na-Sm} + \left(-\frac{7}{2}x + \frac{1}{2}z\right) \text{H}_2\text{O} + \left(-\frac{1}{4}x + \frac{1}{2}y - \frac{1}{4}z\right)\text{O}_2 \rightleftarrows \left(\text{Fe}_x\text{O}_y\text{H}_z\right) / \text{Na-Sm} \tag{1}$$

$$\Delta E = E\left(\left(\text{Fe}_x\text{O}_y\text{H}_z\right) / \text{Na-Sm}\right) - E(\text{Na-Sm}) - xE(\text{Fe complex}) - \left(-\frac{7}{2}x + \frac{1}{2}z\right)E(\text{H}_2\text{O}) - \left(-\frac{1}{4}x + \frac{1}{2}y - \frac{1}{4}z\right)E(\text{O}_2) \tag{2}$$

$$\Delta G(T,p) = \frac{1}{A}\left[\Delta E - \left(-\frac{7}{2}x + \frac{1}{2}z\right)\Delta\mu_{\text{H}_2\text{O}} - \left(-\frac{1}{4}x + \frac{1}{2}y - \frac{1}{4}z\right)\Delta\mu_{\text{O}_2}\right] \tag{3}$$

$$\Delta\mu_{\mathrm{gas}} = \Delta\mu_{\mathrm{gas}}(T, p^0) + RT \ln\left(\frac{p_{gas}}{p^0}\right) \qquad (\mathrm{gas} = \mathrm{H_2O\ and\ O_2}) \tag{4}$$

where $Fe_xO_yH_z$ refers to the structures of the five types of aqua–Fe(III) species considered in this study which are encapsulated in the $Al_{20}Si_{28}O_{96}H_{20}$. $E(Fe_xO_yH_z/\text{Na-Sm})$ is the total energy of these species, E(Na-Sm) is the total energy of the smectite model structure ($Al_{20}Si_{28}O_{96}H_{20}$), E(Fe complex) is the total energies of isolated Fe complex species, and $E(H_2O)$ is the total energy of the isolated H_2O molecule. T is the temperature (K), p^0 is the atmospheric pressure, p_{gas} is the partial pressure of H_2O and O_2 gases, and $\Delta\mu_{\mathrm{gas}}$ is the change in the chemical potential of H_2O and O_2 gases.

References

1 B. Ravel and M. Newville, *J. Synchrotron Radiat.*, 2005, **12**, 537–541.

2 G. Kresse and J. Hafner, *Phys. Rev. B Condens. Matter*, 1994, **49**, 14251–14269.

3 G. Kresse and J. Furthmüller, *Comput. Mater. Sci.*, 1996, **6**, 15–50.

4 P. E. Blöchl, *Phys. Rev. B Condens. Matter*, 1994, **50**, 17953–17979.

5 J. P. Perdew, K. Burke and M. Ernzerhof, *Phys. Rev. Lett.*, 1996, **77**, 3865–3868.

6 S. Grimme, J. Antony, S. Ehrlich and H. Krieg, *J. Chem. Phys.*, 2010, **132**, 154104.

7 S. Grimme, S. Ehrlich and L. Goerigk, *J. Comput. Chem.*, 2011, **32**, 1456–1465.

8 S. Yasumura, H. Ide, T. Ueda, Y. Jing, C. Liu, K. Kon, T. Toyao, Z. Maeno and K. Shimizu, *JACS Au*, 2021, **1**, 201–211.

9 M. W. Chase and A. F. Jan, *Journal of physical and chemical reference data*, 1985, **14**, 1856.

Tables and Figures

Table S1. The composition of different materials.

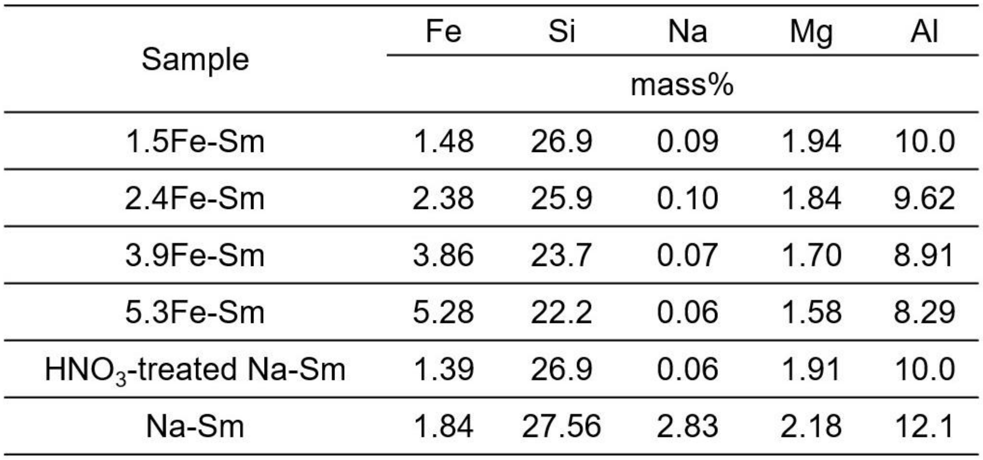

Sample	Fe	Si	Na	Mg	Al
			mass%		
1.5Fe-Sm	1.48	26.9	0.09	1.94	10.0
2.4Fe-Sm	2.38	25.9	0.10	1.84	9.62
3.9Fe-Sm	3.86	23.7	0.07	1.70	8.91
5.3Fe-Sm	5.28	22.2	0.06	1.58	8.29
HNO_3-treated Na-Sm	1.39	26.9	0.06	1.91	10.0
Na-Sm	1.84	27.56	2.83	2.18	12.1

Table S2. Result of the curve-fitting analysis of Fe K-edge EXAFS spectrum of 5.3Fe-Sm.

Sample	Shell	Coordination number	Bond distance / Å	Debye-Waller factor / $Å^{-2}$	Residual factor / %
5.3Fe-Sm	Fe–O	2.1	1.92	0.007	0.8
	Fe–O	4.1	2.04	0.005	
	Fe–O	0.7	2.32	0.010	

Table S3. Calculated relative energies (based on DFT) of aqua–Fe(III) species within a Al$_{20}$Si$_{28}$O$_{96}$H$_{20}$ matrix and containing Fe(III) in different spin states.

Chemical formula of aqua-Fe(III)	Structure of aqua-Fe(III) in the Al$_{20}$Si$_{28}$O$_{96}$H$_{20}$	Spin multiplicity^a	Magnetism	Spin Fe1	Spin Fe2	ΔE (eV)
[Fe^{III}(OH)(H$_2$O)$_3$]	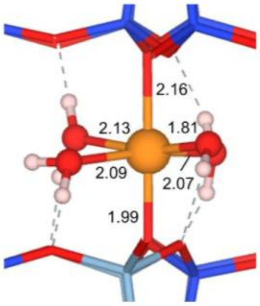	1/2 (Low spin)	Ferro.	1.02	-	1.63
		3/2 (Intermediate spin)	Ferro.	3.11	-	0.75
		5/2 (High spin)	**Ferro.**	**4.35**	**-**	**0.00**
[(H$_2$O)$_2$Fe^{III}O$_2$Fe^{III}(H$_2$O)$_2$]	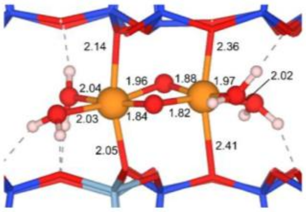	1/2 (Low spin)	Ferro.	3.04	-1.05	1.30
			Anti.		Unstable^b	
		3/2 (Intermediate spin)	Ferro.	3.10	3.18	0.62
			Anti.		Unstable^b	
		5/2 (High spin)	Ferro.	4.29	4.35	0.05
			Anti.	**4.26**	**-4.32**	**0.00**
[(H$_2$O)$_2$Fe^{III}(OH)$_2$Fe^{III}(H$_2$O)$_2$]	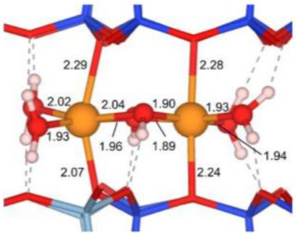	1/2 (Low spin)	Ferro.	1.04	1.15	3.04
			Anti.		Unstable^b	
		3/2 (Intermediate spin)	Ferro.	3.12	3.59	1.14
			Anti.		Unstable^b	
		5/2 (High spin)	Ferro.	4.41	4.40	0.04
			Anti.	**4.39**	**-4.38**	**0.00**

^{a}The spin multiplicity values listed in the table were used as the initial settings for the calculations. ^{b}The calculations did not converge with the specified spin states.

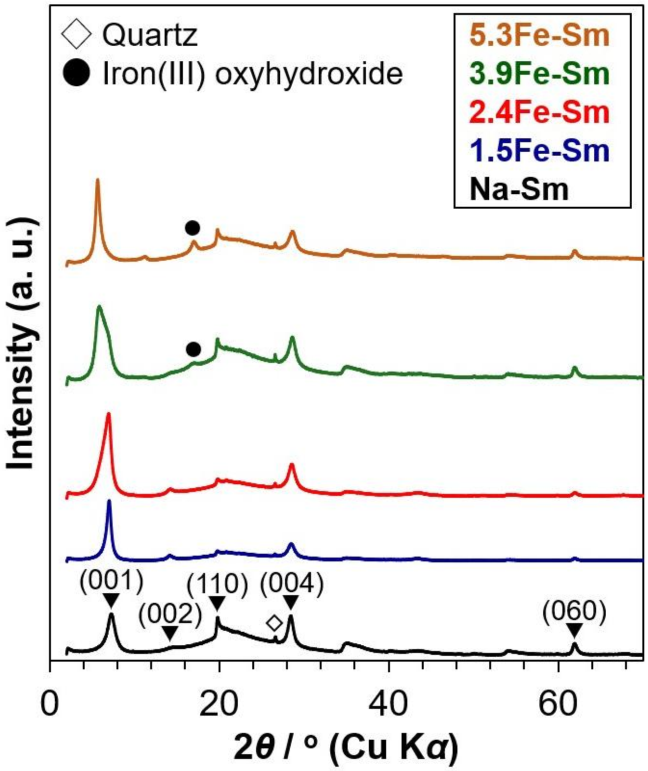

Fig. S1. Wide-angle XRD patterns of different materials.

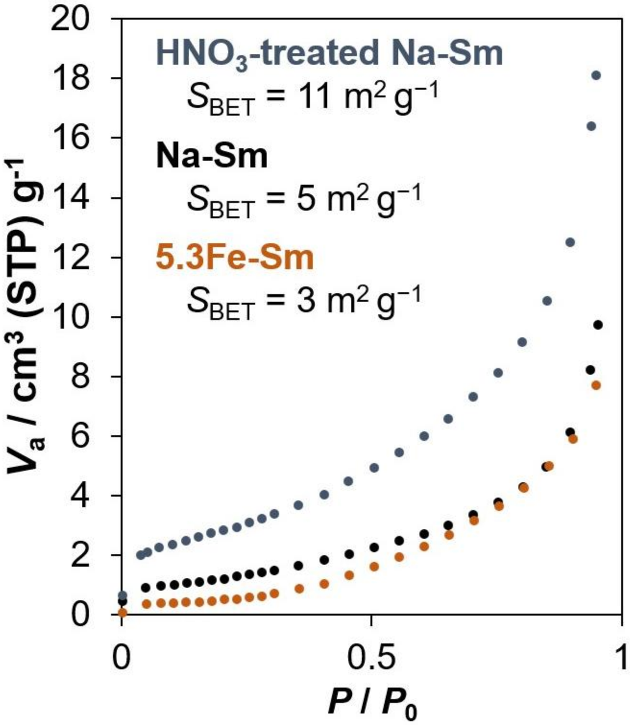

Fig. S2. N_2 adsorption isotherms of different materials.

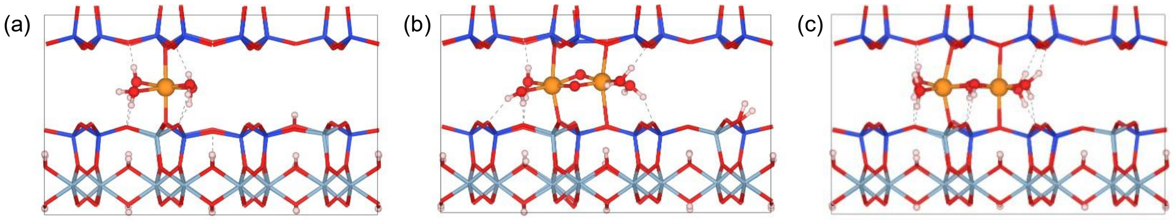

Fig. S3. DFT-determined structures of aqua–Fe(III) species in smectite model structure ($Al_{20}Si_{28}O_{96}H_{20}$), (a) [$Fe^{III}(OH)(H_2O)_3$], (b) [$(H_2O)_2Fe^{III}O_2Fe^{III}(H_2O)_2$] and (c) [$(H_2O)_2Fe^{III}(OH)_2Fe^{III}(H_2O)_2$].